J Chem Crystallogr (2013) 43:412–420
DOI 10.1007/s10870-013-0438-6

ORIGINAL PAPER

The Synthesis, X-ray Structure Analysis, and Photoisomerization Assessment of the Acyclic Triazenes 4-[(*E*)-2-(biphenyl-4-yl)diazenyl]-morpholine and 1,3-Bis(biphenyl-4-yl)triazene

Carolyn Mukai · Emanuel Zamora · Jillian L. Blatti · Frank R. Fronczek · Ralph Isovitsch

Received: 27 March 2013 / Accepted: 10 July 2013 / Published online: 23 July 2013

Abstract The acyclic triazenes 4-[(*E*)-2-(biphenyl-4-yl)diazenyl]-morpholine (**1**) and 1,3-bis(biphenyl-4-yl)triazene (**2**) were prepared and their X-ray crystal structures determined. Compound **1** crystallized in the monoclinic space group $P2_1/c$ with $a = 29.153$ (5) Å, $b = 6.0444$ (14) Å, $c = 7.5997$ (15) Å, and $\beta = 96.03$ (1)°. Compound **2** crystallized as the 1/4 cyclohexane solvate in the triclinic space group $P\bar{1}$ with $a = 10.3228$ (10) Å, $b = 13.4541$ (14) Å, $c = 15.4323$ (15) Å, $\alpha = 87.158$ (4)°, $\beta = 76.030$ (4)° and $\gamma = 71.492$ (5)°. The N–N double bond in **1** and **2** adopted an (*E*)-configuration and had bond angles that ranged from 112.19 (9)° to 114.01 (13)°, which deviated from optimal trigonal planar geometry by 6°–8°. A degree of π-conjugation across the acyclic triazene moieties in compounds **1** and **2** was indicated by N–N double and single bond lengths that were respectively longer and shorter than the literature values for these types of bonds. The room temperature electronic absorption spectra of **1** and **2** in various solvents were both dominated by an intense band above 300 nm that was assigned to a combination of $\pi \rightarrow \pi^*$ and $n \rightarrow \pi^*$ transitions. Compounds **1** and **2** in acetonitrile and methanol solution were found to undergo *trans* → *cis* photoisomerization. The magnitudes of *trans* → *cis* rate constants were rationalized in terms of the degree of solvent stabilization of the dipolar resonance hybrid structure of the acyclic triazene subunits in **1** and **2**. Irradiation of chloroform solutions of **1** and **2** caused *trans* → *cis* photoisomerization and radical decomposition to occur.

Keywords Acyclic triazenes · X-ray structures · Electronic absorption spectra · Photoisomerization

Introduction

Acyclic triazenes are an enormous class of useful molecules that share one common characteristic: they all contain three successive nitrogen atoms whose bonding is similar to that found in an allylic group, for example, RN=N–NR′R″ as compared to H_2C=CH–CR. Acylic triazenes can be prepared using a variety of synthetic methodologies, with the usual route being a coupling reaction between an aryl diazonium ion and a primary or secondary amine [1, 2]. The coupling of an aryl diazonium ion to a Grignard or alkyllithium reagent has also been used to prepare acyclic triazenes [3]. A recently developed synthetic methodology that gave acyclic triazenes in high yields involved the reaction of organic azides with neutral *N*-heterocyclic carbenes [4].

Research into the application of acyclic triazenes to a wide variety of areas is ongoing [5]. The ease at which they can be transformed into amines and their stability under a variety of conditions makes them attractive protecting groups for aniline derivatives [6]. Acyclic triazenes have been used in the synthesis of novel heterocyclic compounds. For example, they have served as both linker and synthon in the solid-phase synthesis of substituted benzopyridazines as well as precursors for the preparation of aryl-1H-benzotriazoles [7, 8]. In the area of medicinal

---

Electronic supplementary material The online version of this article (doi:10.1007/s10870-013-0438-6) contains supplementary material, which is available to authorized users.

C. Mukai · E. Zamora · J. L. Blatti · R. Isovitsch (✉)
Department of Chemistry, Whittier College,
13406 Philadelphia Street, Whittier, CA 90608, USA
e-mail: risovits@whittier.edu

F. R. Fronczek
Department of Chemistry, Louisiana State University,
Baton Rouge, LA 70803, USA

chemistry the use of acyclic triazenes as cancer-fighting drugs that function as DNA alkylating agents has been explored [9]. Work in materials chemistry research has utilized acyclic triazenes with unique aromatic moieties to derivatize silicon surfaces and carbon nanotubes [10, 11]. The conjugation of acyclic triazenes and their ability to undergo photophysical and thermal isomerization has been exploited in the synthesis of donor–acceptor complexes and redox-active compounds [12, 13].

Our research seeks a better understanding of the bonding and photophysical properties of acyclic triazenes toward the goal of increasing their thermal stability and predictably controlling their *trans* → *cis* photoisomerization for their eventual incorporation into photochromic devices. Toward this end, we present the syntheses and X-ray structures of an asymmetric and symmetric acyclic triazene, both of which were prepared from 4-aminobiphenyl (**1** and **2**, Scheme 1). The *trans* → *cis* photoisomerization behavior of **1** and **2** in various solvents is also discussed.

Experimental

Reagents and Techniques

Synthetic procedures were carried out using standard techniques. Solvents and reagents were purchased from Sigma-Aldrich or Acros Organics and used as received. Melting points were determined in open capillaries and are uncorrected. ^{1}H and ^{13}C NMR spectra were recorded on a JEOL ECX 300 MHz spectrometer from DMSO-d_6, $CDCl_3$, acetone-d_6, and CD_2Cl_2 solutions using TMS as the internal standard. The data from ^{1}H and ^{13}C NMR spectra of compounds **1** and **2**, respectively measured in DMSO-d_6 and $CDCl_3$ solution, are listed below. These solvents resulted in the best spectra in terms of larger chemical shift difference between neighboring proton and carbon resonances. Care was taken to exclude light from all NMR samples. IR spectra were recorded as KBr disks on a Perkin Elmer Spectrum 1 FT-IR. Electronic absorption spectra were obtained on a Hewlett Packard 8453 diode array spectrometer. M-H-W Laboratories of Tucson, Arizona performed the elemental analyses in this work.

Determination of Observed First Order *trans* → *cis* Photoisomerization Rate Constants for Compounds **1** and **2**

Observed first order *trans* → *cis* photoisomerization rate constants (k_{obs}) are reported as an average of three independent trials with standard deviations. They were obtained by monitoring the disappearance of the *trans* isomer over time via the decrease in absorbance of the longest wavelength maximum in its electronic absorption spectrum [14]. Concentration of the *trans* isomer at time *t* was obtained from a calibration curve of the *trans* isomer. Calibration curves of the *trans* isomers had R^2 values that ranged from 0.9955 to 0.9973. Plots of ln [*trans* isomer] versus time were linear ($R^2 = 0.9951$–0.9997), with the slopes of the lines being taken as *trans* → *cis* k_{obs}.

Photoisomerization experiments were done with stirred, room temperature, argon-bubbled solutions of **1** and **2** in a quartz cuvette using the apparatus depicted in Fig. S1 in the Supplementary Materials. Solutions of **1** and **2** were approximately 2×10^{-5} M and prepared using spectrophotometric grade acetonitrile, chloroform and methanol. Irradiation was via 16 W commercially available black light fluorescent bulbs, whose output is at wavelengths greater than 300 nm. The black light bulbs were ~6 cm from the sample.

Synthesis of 4-[(*E*)-2-(biphenyl-4-yl)diazenyl]-morpholine (**1**)

0.250 g (1.48 mmol) of 4-aminobiphenyl was added to 1 mL of 6 M HCl and 2 mL of H_2O, and heated for 10 min with stirring to yield an orange-pink suspension. The suspension was cooled to 0 °C, diluted with 1 mL of H_2O, and then an aqueous solution of $NaNO_2$ (0.104 g (1.55 mmol) in 1 mL of H_2O) was added dropwise over 10 min with stirring. The reaction mixture turned a clear yellow-orange color. It was allowed to stir for 20 min, and became slightly green. Next,

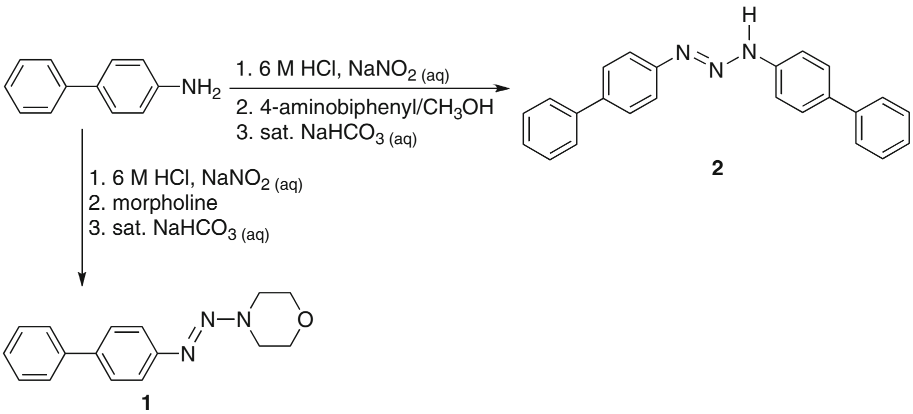

Scheme 1 The syntheses of compounds **1** and **2**

0.14 mL (1.60 mmol) of morpholine was added dropwise with stirring over 10 min. The reaction mixture formed a pale yellow precipitate. The reaction mixture was stirred for 20 min, and 4 mL of H_2O and ~40 mL of 10 % aqueous $NaHCO_3$ were added to bring the reaction mixture to pH 8. The crude product was collected over vacuum filtration, washed well with H_2O, and allowed to air dry. Taking care to exclude direct light, the crude product was recrystallized twice from a 1:3 cyclohexane-petroleum ether mixture to give 0.0798 g (31 %) of beige crystalline flakes of pure **1**. MP 110–111 °C; IR (KBr pellet) 3059, 3031, 2976, 2873, 1460, 1385, 1349, 1144, 1102, 1011, 836, 761 cm^{-1}; ^1H NMR (300 MHz, DMSO-d_6) ppm 7.63 (d), 7.42 (d), 7.31 (m), 3.73 (m); ^{13}C NMR (75 MHz, DMSO-d_6) ppm 149.6, 140.1, 138.3, 129.5, 127.8, 126.9, 121.5, 66.1, 49.1 (br. s); EI-HR-MS: *m/z* for $[M+H]^+ = 268.1446$, Calcd. *m/z* for $[M+H]^+ = 268.1450$ *Anal* Calcd. For $C_{16}H_{17}N_3O$ (267.4): C 71.87, H 6.42, N 15.72. Found: C 71.99, H 6.27, N 15.83.

Synthesis of 1,3-Bis(biphenyl-4-yl)triazene (**2**)

0.250 g (1.48 mmol) of 4-aminobiphenyl was added to 1 mL of 6 M HCl and 2 mL of H_2O and heated on a hot plate for 10 min with stirring to yield an orange-pink suspension. The suspension was cooled to 0 °C and 1 mL of H_2O added. The suspension was maintained at 0 °C and a solution of 0.104 g (1.55 mmol) $NaNO_2$ in 1 mL of H_2O was added drop wise with stirring over 10 min. The reaction mixture was stirred for 20 min and turned a clear orange-yellow color. Next, a solution of 0.275 g (1.63 mol) of 4-aminobiphenyl in 5 mL of CH_3OH was added drop wise with stirring over 10 min. After stirring for 20 min, the reaction mixture formed an off-white precipitate. To this, 4 mL of H_2O and ~40 mL of 10 % aqueous $NaHCO_3$ were added to bring the reaction mixture to pH 8. Upon addition of the $NaHCO_3$, the reaction mixture foamed and produced a dark yellow precipitate that was collected over vacuum filtration, washed well with H_2O, and allowed to air dry. While taking care to exclude direct light, the crude product was recrystallized from cyclohexane. 0.153 g (59 %) of dark brown needles of pure **2** were obtained. MP 140–141 °C; IR (KBr pellet) 3029, 2922, 2846, 1608, 1532, 1484, 1430, 1384, 1252, 1205, 765, 698 cm^{-1}; ^1H NMR (300 MHz, $CDCl_3$) ppm 9.78 (s), 7.63 (m), 7.49 (m), 7.36 (m); ^{13}C NMR (75 MHz, $CDCl_3$) ppm 144.4 (br. s) 140.6, 139.8, 129.0, 128.1, 127.3, 127.0, 118.0 (br. s); EI-HR-MS: *m/z* for $[M+H]^+ = 350.1647$, Calcd. *m/z* for $[M+H]^+ = 350.1657$ *Anal* Calcd. For $C_{24}H_{19}N_3$ (349.5): C 82.48, H 5.49, N 12.03. Found: C 82.37, H 5.60, N 11.88.

X-ray Structure Determination

X-ray quality crystals of **1** and **2** were used for data collection at T = 90 K. The data for **1** and **2** were collected on a Bruker Kappa APEX-II CCD diffractometer equipped with an Oxford Cryosystems Cryostream chiller and graphite-monochromated Cu *Kα* radiation ($\lambda = 1.54178$ Å). For compound **1**, a total of 9,226 measured reflections with $\theta_{max} = 68.5°$ yielded 2,392 unique data, and for compound **2** a total of 20,672 measured reflections with $\theta_{max} = 68.8°$ yielded 6,852 unique data. Structures were solved by direct methods, and structure refinements were carried out using SHELXL-97 [15]. All H-atoms were visible in difference maps, but were placed in idealized positions during refinement, except for the NH hydrogen atom in **2**, for which coordinates were refined.

CCDC 891358 and 891359 contain the supplementary crystallographic data for this paper. These data can be obtained free of charge from the Cambridge Crystallographic Data Centre via http://www.ccdc.cam.ac.uk/products/csd/request/.

Results and Discussion

Synthesis and Characterization of Compounds **1** and **2**

4-Aminobiphenyl in 6 M HCl was combined with an aqueous solution of $NaNO_2$ to yield a diazonium ion that underwent coupling with morpholine and with 4-aminobiphenyl to yield compounds **1** and **2**, respectively (Scheme 1) [16, 17]. Variable low to moderate yields of **1** (9–38 %) and **2** (34–59 %) were obtained, which was explained by the diazonium ion more readily participating in electrophilic aromatic substitution with the electron-rich terminal ring of a neighboring biphenyl moiety rather than undergoing coupling [18].

Different analytical techniques were used to confirm the identity of **1** and **2**. While the NMR spectra of both compounds offered valuable insights into their structures, such as the resonances at 66.1 and 49.1 ppm in the ^{13}C NMR spectrum of **1** that were assigned to the morpholine carbons, and the singlet at 9.78 ppm in the ^1H NMR spectrum of **2** that was assigned to the proton of the acyclic triazene subunit, they did exhibit anomalous behavior [19, 20].

The ^1H NMR spectra of both compounds had integrals that were different from the predicted values by ±1 hydrogen atom. This observed discrepancy may be caused by different rotamers and conformers of **1** and **2** that exist in solution. Both of these phenomena would cause the hydrogen atoms of compounds **1** and **2** to be in slightly different environments, resulting in integrals that were slightly off from the expected values [17, 18, 21]. The integrals in the ^1H NMR spectra of both compounds were observed to be lower or higher than expected when obtained from DMSO-d_6, $CDCl_3$, acetone-d_6, and CD_2Cl_2 solution.

The existence of rotamers and conformers of **1** and **2** in solution was supported by the presence of broad singlets in the ^{13}C NMR spectra of both [17, 21]. The missing resonance in the ^{13}C NMR spectrum of **1** was rationalized in terms of the signals from two carbon atoms with small chemical shift differences being obscured by a broadened peak.

High-resolution mass spectroscopy and elemental analysis of **1** and **2** supported their identity and purity. Both compounds had HR–ESI–MS that exhibited $[M+H]^+$ peaks at $m/z = 268.1446$ and 350.1647, respectively. These values were both within 3 ppm of the calculated ones for each compound. Compounds **1** and **2** both yielded acceptable elemental analyses.

Crystallographic Study

Crystal and structure refinement data for compounds **1** and **2** are presented in Table 1, while selected bond lengths and angles for both compounds are in Table 2. The *ORTEP* representation of **1** is shown in Fig. 1, and that of **2** is shown in Fig. 2.

The asymmetric unit of compound **2** consisted of two independent molecules of **2** that had essentially equal bond

Table 1 Crystal and experimental data for compounds **1** and **2**

Compound	1	2
Empirical formula	$C_{16}H_{17}N_3O$	$C_{24}H_{19}N_3 \cdot 0.25(C_6H_{12})$
Formula weight	267.33	370.46
CCDC deposition no.	891358	891359
Space group	Monoclinic, $P2_1/c$	Triclinic, $P\bar{1}$
Crystal dimension (mm^3)	0.34 × 0.33 × 0.04	0.30 × 0.20 × 0.15
Unit cell parameters		
a	29.153 (5) Å	10.3228 (10) Å
b	6.0444 (14) Å	13.4541 (14) Å
c	7.5997 (15) Å	15.4323 (15) Å
α		87.158 (4)°
β	96.03 (1)°	76.030 (4)°
γ		71.492 (5)°
V	1331.8 (5) Å^3	1971.5 (3) Å^3
Temperature (K)	90	90
Z	4	4
D_c (Mg m^{-3})	1.333	1.248
Radiation	CuKα	CuKα
μ (CuKα) (mm^{-1})	0.68	0.57
$F(000)$	568	784
θ_{max}	68.5°	68.8°
Index ranges	$-31 \leq h \leq 34$	$-10 \leq h \leq 11$
	$-7 \leq k \leq 7$	$-16 \leq k \leq 15$
	$-8 \leq l \leq 9$	$-18 \leq l \leq 18$
R_{int}	0.033	0.027
Goodness of fit on F^2	1.06	1.02
Reflections collected	9,226	20,672
Independent reflections	2,392	6,852
Reflections with $I > 2\sigma(I)$	2,262	5,763
Refined parameters	182	530
R_1/wR_2	0.034/0.088	0.041/0.109
Measurement	Bruker APEX-II CCD diffractometer	Bruker APEX-II CCD diffractometer
Refinement	Full-matrix least squares method on F^2	Full-matrix least squares method on F^2
Extinction coefficient	0.0014 (2)	–
$(\Delta\rho)_{max}$, $(\Delta\rho)_{min}$	0.23, −0.19 e Å^{-3}	0.24, −0.17 e Å^{-3}

lengths and angles, as well as one-half of a molecule of cyclohexane.

The acyclic triazene subunits of compounds **1** and **2** were found to have similar structural characteristics. The N–N double bonds in **1** and **2** adopted an (*E*)-configuration. The bond angles of the N–N double bond in both compounds deviated from optimal trigonal planar geometry by 6°–8°. For example, compound **1** had a N3–N2–N1 bond angle of 113.78 (9)° and a N2–N3–C5 bond angle of 112.19 (9)°, and compound **2** had a N1–N2–N3 bond angle of 114.01 (13)° and a N2–N1–C1 bond angle of 113.32 (13)°. The geometry and bond angles of the N–N double bond in **1** and **2** are similar to those of related acyclic triazenes [22, 23].

Deviations from the literature bond length values for a N–N double bond (1.222 Å) and a N(sp^2)–N(sp^3) single bond (1.420 Å) indicated a degree of π-conjugation across the acyclic triazene moieties in compounds **1** and **2** [24]. For example, the N–N double bond in **1** (N2–N3) was longer than expected with a length of 1.2660 (14) Å. Conversely, the N–N single bond (N1–N2) was shorter than expected with a length of 1.3620 (13) Å. The same deviations from the ideal were observed in compound **2** with a N–N double bond (N1–N2) length of 1.2891 (18) Å and a N–N single bond (N1–N2) length of 1.3109 (19) Å. Compound **2** had a greater degree of delocalization than compound **1** in its acyclic triazene moiety, as indicated by its more similar N–N bond lengths.

Table 2 Selected bond lengths (Å) and angles (°) for compounds **1** and **2**

1			
C12–C13	1.3880 (16)	C11–C12	1.3999 (16)
C8–C11	1.4886 (15)	C7–C8	1.3965 (17)
C6–C7	1.3831 (16)	N3–C5	1.4306 (14)
N2–N3	1.2660 (14)	N1–N2	1.3620 (13)
N1–C3	1.4686 (14)	C3–C4	1.5164 (15)
O1–C4	1.4341 (14)	C13–C12–C11	120.60 (11)
N2–N3–C5	112.19 (9)	N3–N2–N1	113.78 (9)
N2–N1–C3	111.84 (8)	N2–N1–C2	119.39 (9)
N1–C3–C4	109.21 (9)	O1–C4–C3	111.04 (9)
C2–N1–C3	114.64 (8)		
2			
C8–C9	1.377 (2)	C7–C8	1.402 (2)
C4–C7	1.473 (2)	C2–C3	1.377 (2)
C1–C2	1.386 (2)	N1–C1	1.415 (2)
N1–N2	1.2891 (18)	N2–N3	1.3109 (19)
N3–C13	1.416 (2)	C35–C36	1.387 (2)
C31–C36	1.396 (2)	C28–C31	1.491 (2)
C29–C30	1.383 (2)	C25–C30	1.392 (2)
N4–C25	1.4155 (19)	N4–N5	1.3070 (19)
N5–N6	1.2898 (18)	N6–C37	1.422 (2)
N2–N1–C1	113.32 (13)	N1–N2–N3	114.01 (13)
N2–N3–C13	117.28 (14)	C3–C2–C1	121.18 (15)
C9–C8–C7	120.93 (16)	N5–N4–C25	116.93 (13)
N6–N5–N4	114.13 (13)	N5–N6–C37	113.35 (13)

Additional evidence for π-conjugation in the triazene subunits of **1** and **2** was observed. The bond angles of the morpholine nitrogen atom (N1) in **1** were observed to be 111.84 (8), 114.64 (8) and 119.39 (9)°. These bond angles indicate the partial sp^2 character of N1 and its participation in π-delocalization with N2–N3. Conjugation of the triazene moiety (N1–N2–N3) with a phenyl ring (C1–C6) in **2** was indicated by the 1.415 (2) Å length of N1–C1, which was somewhat shorter than the literature value of 1.431 Å for a C$_{\text{aryl}}$–N bond [24]. π-Delocalization of the type observed in compounds **1** and **2** has been observed in similar acyclic triazenes [25–27].

In general, the bond lengths and angles of compounds **1** and **2** corresponded well to related compounds in the literature [19, 22–28].

The packing interactions of **1** are show in Fig. 3. Crystals of **1** were composed of stacks of individual molecules of **1** engaged in short-contact N···H and π···π van der Waal's interactions. Neighboring stacks of **1** participated in weak intermolecular C–H···O hydrogen bonding between a morpholine hydrogen atom (C1–H1A) and a morpholine oxygen atom (O1) with a H···O distance of ~2.57 Å, a C1–O1 distance of 3.507 (2) Å, and a C1–H1A···O1 bond angle of 158° [29].

The main packing interactions of compound **2** involved two molecules of **2** participating in intermolecular N–H···N hydrogen bonding via their triazene subunits. The first hydrogen bond occurred between N1 and the hydrogen bonded to N4, and had a H···N distance of 2.14(2) Å, a N1···N4 distance of 3.036 (2) Å, and a N1···H4N–N4 bond angle of 175.7 (16)°. The second occurred between N6 and the hydrogen bonded to N3, and had a H···N distance of 2.24(2) Å, a N6···N3 distance of 3.153 (2) Å, and a N1···H4N–N4 bond angle of 171.9 (16)° [30]. The two molecules thus formed a hydrogen-bonded dimer of graph set $R_2^2(8)$ [31].

Electronic Absorption Spectroscopy

NMR samples of compounds **1** and **2** in DMSO-d_6, CDCl$_3$, acetone-d_6, and CD$_2$Cl$_2$ solution were observed to undergo color changes when left out on the bench top and exposed to ambient light in the laboratory over a period of 24 h. This observation prompted an investigation of the electronic absorption spectra of both compounds in a polar aprotic, a polar protic, and moderately polar solvent (acetonitrile, methanol and chloroform, respectively). Electronic absorption data for compounds **1** and **2** are summarized in Table 3.

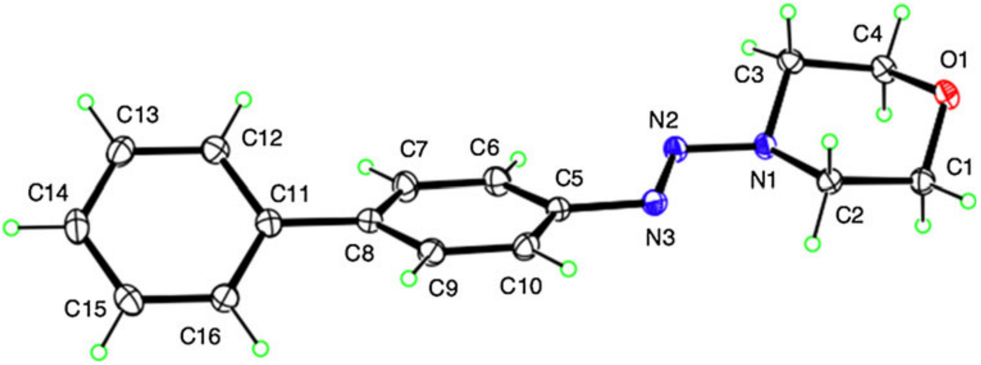

Fig. 1 *ORTEP* view of compound **1**. *Ellipsoids* are represented at the 50 % probability level

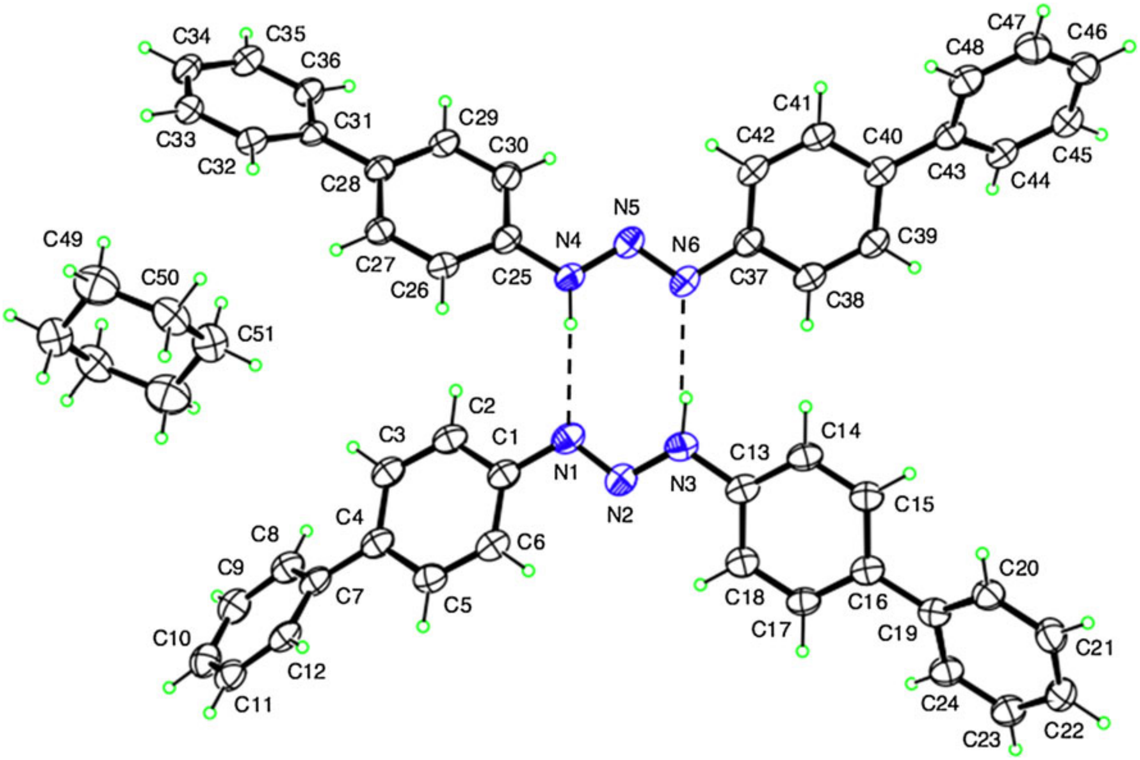

Fig. 2 *ORTEP* view of compound **2** with intermolecular N–H···N hydrogen bonding emphasized. *Ellipsoids* are represented at the 50 % probability level

Compounds **1** and **2** have electronic absorption spectra that were insensitive to solvent polarity and hydrogen-bonding ability. A single, intense band dominated the spectra of both compounds. In compound **1,** this band was at ~330 nm ($\varepsilon = 18{,}600$–$20{,}000$ L mol^{-1} cm^{-1}) and in compound **2** at ~375 nm ($\varepsilon = 25{,}400$–$28{,}300$ L mol^{-1} cm^{-1}). The intensities of these bands, as indicated by their molar extinction coefficients, suggested that they arise from a $\pi \rightarrow \pi^*$ transitions [32, 33]. A recent computational investigation by Jacquemin and coworkers on a series of acyclic triazenes revealed that the origin of this band is more likely a combination of $\pi \rightarrow \pi^*$ and $n \rightarrow \pi^*$ transitions [34]. They indicated that these two transitions would be observable in the spectra of acyclic triazenes that were unsymmetrically substituted with groups of differing electron-donating or accepting character as a broadened asymmetric band at wavelengths greater than 300 nm. This is the case with compound **1**, with its maximum at ~330 nm and a shoulder at 305 nm ($\varepsilon = 17{,}600$–$19{,}100$ L mol^{-1} cm^{-1}). The spectra of compound **2** had less intense absorption bands below 310 nm, which were assigned to $\pi \rightarrow \pi^*$ transitions based on the biphenyl unit [35].

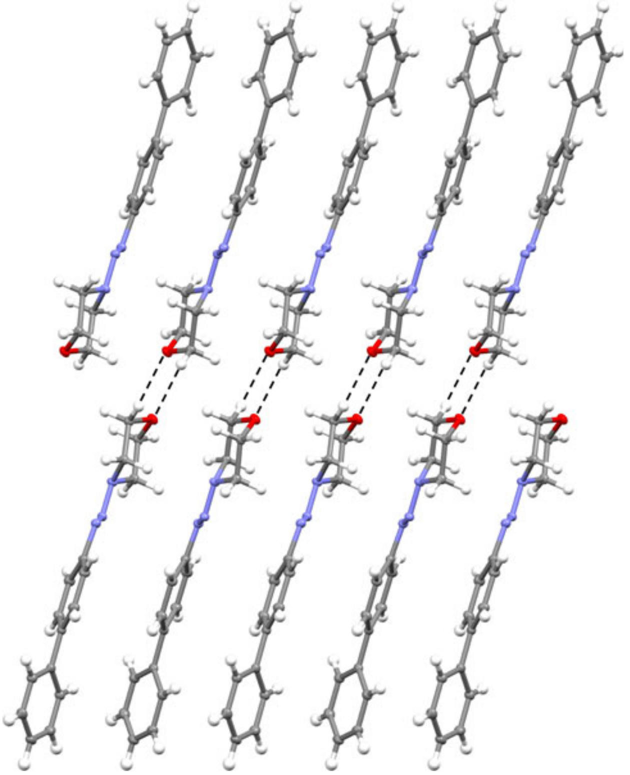

Fig. 3 Crystal packing in compound **1** as viewed along the crystallographic *b*-axis, with intermolecular C–H···O hydrogen bonding emphasized

Table 3 Electronic absorption spectral data for compounds **1** and **2** in various solvents

	$\lambda_{max,abs}$ (nm) (ε)[a]	
	1	**2**
CH_3CN	328 (19,400)	375 (28,200)
	305 (18,400)[b]	304 (11,600)
		267 (15,200)
$CHCl_3$	333 (18,600)	375 (25,400)
	305 (17,600)[b]	304 (10,400)
		266 (17,900)
CH_3OH	325 (20,000)	377 (28,300)
	305 (19,100)[b]	304 (11,300)
		267 (17,300)

Spectra were acquired at room temperature unless otherwise noted

[a] Molar extinction coefficients L mol^{-1} cm^{-1}

[b] Shoulder

trans → *cis* Photoisomerization Studies

While the *trans* → *cis* photoisomerization kinetics of compounds similar to **2** have been investigated, those of compounds related to **1** have not [36, 37]. Irradiation ($\lambda > 300$ nm) of solutions of **1** and **2** resulted in the generation the *cis* isomer [1]. The clear isosbestic points that manifested in the electronic absorption spectra taken during the irradiation of **1** and **2** in acetonitrile and methanol support *trans* → *cis* photoisomerization as the major process. Based on their electronic absorption spectra, thermal isomerization of the *cis* isomer of compounds **1** and **2** back to the *trans* isomer was not observed at ambient conditions.

Irradiation of solutions of **1** and **2** in acetonitrile and methanol led to a decrease in absorbance above 300 nm, and an increase at ~260 nm. The clean separation of these two areas permitted the quantification of the concentration of the *trans* isomer at various times *t* during irradiation. From these data, the *trans* → *cis* k_{obs} could be determined [14]. The processes occurring in irradiated chloroform solutions of **1** and **2** were observed to be more complex.

Table 4 summarizes the first order, observed *trans* → *cis* k_{obs} for **1** and **2** in the aforementioned solvents. The changes that occur in methanol solutions of compounds **1** and **2** during irradiation are illustrated in Figs. 4 and 5. These plots respectively depict the electronic absorption spectra of **1** and **2** at various times *t* during the course of a photoisomerization experiment. Similar plots of acetonitrile and chloroform solutions of **1** and **2** are shown in Figs. S2–S5 in the Supplementary Materials.

Table 4 Observed first order photoisomerization (*trans* → *cis*) rate constants for compounds **1** and **2** in various solvents

	1	**2**
CH_3CN	0.013 ± 0.001	0.034 ± 0.004
$CHCl_3$	Photolytic decomposition	Photolytic decomposition
CH_3OH	0.045 ± 0.004	0.0026 ± 0.0003

Rate constant unit s^{-1}

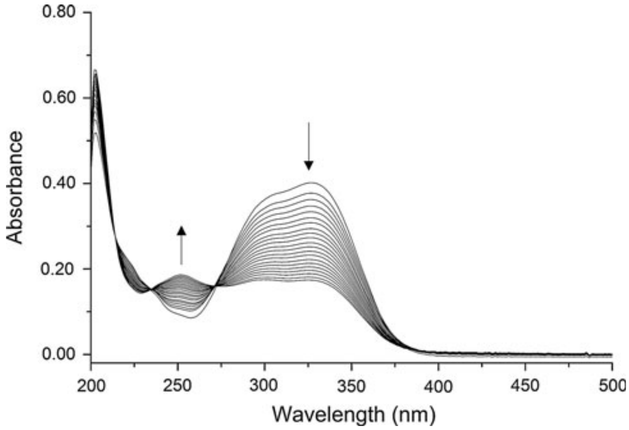

Fig. 4 Electronic absorption spectra of the irradiation of a dilute CH_3OH solution of compound **1** taken at 1-min intervals from 0 to 20 min. Isosbestic points were observed at 235 and 271 nm

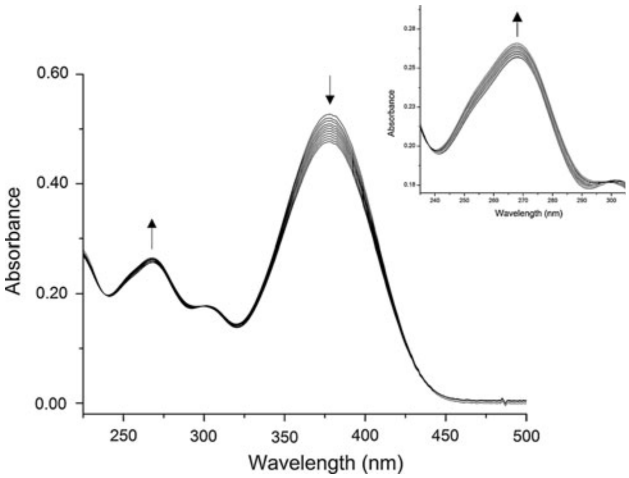

Fig. 5 Electronic absorption spectra of the irradiation of a dilute CH_3OH solution of compound **2** take at 4-min intervals from 0 to 40 min. Isosbestic points were observed at 237 and 301 nm

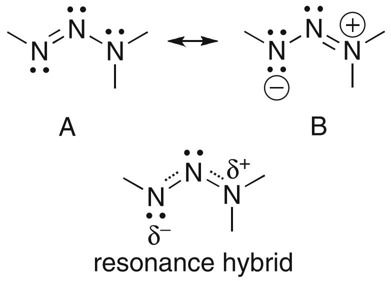

Scheme 2 Resonance representation of the delocalization in the acyclic triazene subunits of compounds **1** and **2**

Resonance structures A and B and their hybrid are shown in Scheme 2 and illustrate the delocalization of the acyclic triazene subunit of compounds **1** and **2**. The trends in *trans* → *cis* k_{obs} can be rationalized in terms of the stabilization of the dipolar hybrid through intermolecular interactions with the solvents used in the irradiation experiments. More effective solvent stabilization of the hybrid results in a greater degree of delocalization and a decreased probability that the triazene will undergo *trans* → *cis* photoisomerization [1, 38, 39]. Solvent effects were seen to be more important than substituent effects as both ends of the acyclic triazene subunits in **1** and **2** were substituted with similar electron-donating groups.

The difference between the *trans* → *cis* k_{obs} for compound **1** in acetonitrile and methanol solutions was slight, with the former approximately three times smaller than the latter. This was rationalized in terms of both solvents only being able to effectively engage in intermolecular interactions with one end of the dipolar acyclic triazene resonance hybrid. Methanol can form hydrogen bonds with the partially negative end, while the linear cyano group of acetonitrile can form dipole–dipole interactions with the sterically crowded and partially positive tertiary nitrogen.

The order-of-magnitude difference between the *trans* → *cis* k_{obs} for compound **2** in acetonitrile and methanol solutions can be understood again in terms of solvent stabilization of the dipolar resonance hybrid. Methanol provided the most stabilization as it is able to hydrogen bond with both ends of the hybrid, while acetonitrile can only form dipole–dipole interactions with the positive end.

The irradiation of a chloroform solution of **1** for 1.5 min resulted in the photobleaching of its absorbance at 333 nm. The irradiation of a chloroform solution of **2** behaved similarly to the irradiations of **2** in acetonitrile and methanol, with its electronic absorption spectra manifesting an isosbestic point at 296 nm. The data from both of these photoisomerization experiments did not behave in a linear fashion, which was attributed to minimal, if any, solvent stabilization of the acyclic triazene linkage. This lack of stabilization is theorized to have resulted in a combination of *trans* → *cis* photoisomerization and radical decomposition processes occurring during irradiation [1, 33].

Conclusions

Two acyclic triazenes, compounds **1** and **2**, were synthesized and their X-ray structures determined. Similarities in the acyclic triazene subunits of compounds **1** and **2** were revealed by their X-ray structures. The N–N double bond in both compounds adopted an (*E*)-configuration and had similar bond angles around the atoms in their acyclic triazene moieties. Both compounds had a degree of delocalization across their acyclic triazene linkages based on N–N double and single bond lengths that were respectively longer and shorter than those values found in the literature. The more similar N–N bond lengths of compound **2** indicated that it had a greater degree of delocalization than compound **1** in its acyclic triazene unit. The packing interactions of **1** consisted of short-contact van der Waal's interactions and intermolecular C–H···O hydrogen bonding. The predominant packing interactions of **2** involved two molecules of **2** participating in intermolecular N–H···N hydrogen bonding. The electronic absorption spectra of both compounds **1** and **2** were insensitive to solvent polarity and hydrogen bonding ability, and were dominated by an intense band above 300 nm that arose from a combination of π → π* and *n* → π* transitions. Both compounds **1** and **2** in methanol and acetonitrile solution underwent *trans* → *cis* photoisomerization, with the rate of this process dependent on the extent of solvent stabilization of the dipolar resonance structure of the acyclic triazene. Irradiation of compounds **1** and **2** in chloroform solution were observed to undergo processes with more complex kinetics.

Acknowledgments Whittier College is acknowledged for support of this research. The upgrade of the diffractometer was made possible by Grant No. LEQSF (2011–2012)-ENH-TR-01, which was administered by the Louisiana Board of Regents. Dr. Simon Jones is thanked for providing HR–ESI–MS of compounds **1** and **2**.

References

1. Fu J, Lau K, Barra M (2009) J Org Chem 74:1770
2. Henry RA, Dehn WM (1943) J Am Chem Soc 65:479
3. Saunders KM, Allen RLM (1985) Aromatic diazo compounds, 3rd edn. Edward Arnold Publishers Ltd, London, p 373
4. Khramov DM, Bielawski CW (2005) Chem Commun 4958
5. Kimball DB, Haley MM (2002) Angew Chem Int Ed Engl 41:3338
6. Gross ML, Blank DH, Welch WM (1993) J Org Chem 58:2104
7. Bräse S, Dahmen S, Heuts J (1999) Tetrahedron Lett 40:6201
8. Kumar RK, Ali MA, Punniyamurthy T (2011) Org Lett 13:2102
9. Wanner MJ, Koch M, Koomen G-J (2004) J Med Chem 47:6875
10. Chen B, Flatt AK, Jian H, Hudson JL, Tour JM (2005) Chem Mater 17:4832
11. Hudson JL, Jian H, Leonard AD, Stephenson JJ, Tour JM (2006) Chem Mater 18:2766
12. Khramov DM, Bielawski CW (2007) J Org Chem 72:9407
13. Ono RJ, Suzuki Y, Khramov DM, Ueda M, Sessler JL, Bielawski CW (2011) J Org Chem 76:3239
14. Moore JW, Pearson RG (1981) Kinetics and mechanism, 3rd edn. Wiley, New York, pp 47–49
15. Sheldrick GM (2008) Acta Cryst A64:112
16. Sengupta S, Bhattacharyya S, Sadhukhan SK (1998) J Chem Soc Perkin Trans 1:275
17. Barra M, Lim H (2006) Trends Org Chem 11:17
18. Carey FA, Sundberg RJ (2000) Advanced organic chemistry, 4th edn. Kluwer Academic/Plenum, New York, p 587
19. Chin T, Phipps A, Fronczek FR, Isovitsch R (2011) J Heterocycl Chem 48:215
20. Chen N, Barra M, Lee I, Chahal N (2002) J Org Chem 67:2271
21. Moser SL, Vaughan K (2004) Can J Chem 82:1725
22. Chin T, Fronczek FR, Isovitsch R (2009) Acta Cryst E65:o3206
23. Hörner M, Brancher AL, Silva A, Borhinhao J, Mössmer CM (2004) Acta Cryst C60:o303
24. Allen FH, Kennard O, Watson DG, Brammer L, Orpen AG, Taylor R (1987) J Chem Soc Perkin Trans 2:S1
25. Hörner M, Bresolin L, Borhinhao J, Hartmann E, Strähle J (2003) Acta Cryst C59:o426
26. Little VR, Jenkins H, Vaughan K (2008) J Chem Crystallogr 38:447
27. Zhang D-C, Fei Z-H, Zhang T-Z, Zhang Y-Q, Yu K-B (1999) Acta Cryst C55:102
28. Jasinski JP, Golen JA, Siddaraju BP, Narayana B, Yathirajan HS (2012) Acta Cryst E68:o362
29. Steiner T (2002) Angew Chem Int Ed Engl 41:49
30. Karadayi N, Çakmak S, Obadasoglu M, Büyükūngör O (2005) Acta Cryst C61:o303
31. Etter MC (1990) Acc Chem Res 23:120
32. Párkányi C, Vernin G, Julliard M, Metzger J (1981) Helv Chim Acta 64:171
33. Panitz JC, Lipper T, Stebani J, Nuyken O, Wokaun A (1993) J Phys Chem 97:5246
34. Preat J, Michaux C, Lewalle A, Perpète EA, Jacquemin D (2008) Chem Phys Lett 451:37
35. Murrell JN (1971) The theory of the electronic spectra of organic molecules. Chapman and Hall Ltd, London, p 238
36. Scaiano JC, Chen C, McGarry PF (1991) J Photochem Photobiol A 62:75
37. Baro J, Dudek D, Luther K, Troe J (1983) Ber Bunsenges Phys Chem 87:1155
38. Anet ALF, Ji Z-H (1984) Tetrahedron Lett 25:1419
39. Marullo NP, Mayfield CB, Wagener EH (1968) J Am Chem Soc 90:510